Self-Assembled Poly(4-vinylpyridine)-Surfactant Systems Using Alkyl and Alkoxy Phenylazophenols

ARTICLE *in* MACROMOLECULES · MAY 2008

Impact Factor: 5.8 · DOI: 10.1021/ma800106t · Source: OAI

7 AUTHORS, INCLUDING:

Kristina Kvashnina
European Synchrotron Radiation Facility
93 PUBLICATIONS **653** CITATIONS
SEE PROFILE

Wim Bras
Nederlandse Organisatie voor Wetenschap…
240 PUBLICATIONS **6,252** CITATIONS
SEE PROFILE

G. ten Brinke
University of Groningen
280 PUBLICATIONS **9,409** CITATIONS
SEE PROFILE

Self-Assembled Poly(4-vinylpyridine)−Surfactant Systems Using Alkyl and Alkoxy Phenylazophenols

Joost de Wit,[†] Gert Alberda van Ekenstein,[†] Evgeny Polushkin,[†] Kristina Kvashnina,[‡] Wim Bras,[‡] Olli Ikkala,[§] and Gerrit ten Brinke*

Laboratory of Polymer Chemistry, Zernike Institute for Advanced Materials, University of Groningen, Nijenborgh 4, 9747 AG Groningen, The Netherlands; Dubble CRG/ESRF, Netherlands Organization for Scientific Research (NWO), c/o ESRF, BP 220, F-38043 Grenoble Cedex, France; and Department of Engineering Physics and Mathematics and Center for New Materials, Helsinki University of Technology, P.O. Box 2200, FIN-02015 HUT Espoo, Finland

Received January 15, 2008; Revised Manuscript Received April 2, 2008

ABSTRACT: Para-substituted alkyl and alkoxy phenylazophenols (PAP's) have been synthesized and used as hydrogen-bonded side chains for poly(4-vinylpyridine)-based comb-shaped supramolecules akin to the well-studied poly(4-vinylpyridine)/pentadecylphenol systems. In this paper we report the self-assembly of these new materials as investigated by DSC and simultaneous SAXS/WAXS. The systems exhibit smectic ordering with a periodicity in the range of 3.0−4.2 nm. The periodicity length scale, the order−disorder transition temperature (T_{ODT}), and the glass transition temperature T_g of the self-assembled systems all increase with increasing alkyl chain length. The correlation between T_{ODT} and T_g observed is argued to be the consequence of the increasing segregation in the self-assembled systems with increasing alkyl tail length of the amphiphiles.

Introduction

During the past decades many different polymer-based responsive materials have been introduced.[1–5] Such materials are of interest because they have the capability to respond to thermal, electrical, electromagnetic, or pH changes, e.g., by undergoing a phase transition. Their applications can be found in drug release systems,[6–8] microfluidics,[9–13] sensor systems,[14–17] etc. A group of materials that holds a great promise in this respect is based on azo-functional polymers, where the presence of azobenzene moieties makes the chain conformations susceptible to photoinduced motions.[18–26] In previous studies we discussed in detail the self-assembly of comb-shaped supramolecules obtained by pentadecylphenol (PDP) amphiphiles hydrogen bonded to poly(4-vinylpyridine) (P4VP).[27,28] Conceptually, the nanoscale layered structures formed in the P4VP(PDP)$_x$ systems, with x denoting the number of phenol groups relative to the number of pyridine groups, occur due to a delicate balance between two properties: on the one hand, the repulsion between the apolar alkyl tails of PDP and the polar P4VP backbone and, on the other, the hydrogen bonding of the phenolic group to the nitrogen of the pyridine moiety of P4VP. If the alkyl tail of the alkylphenols is too short, self-assembly does not occur, while for e.g. $x = 1.0$ macrophase separation will take place if the alkyl tail is too long. This supramolecular concept has been further applied to polystyrene-*block*-poly(4-vinylpyridine) block copolymers, where hydrogen bonding with PDP results in so-called structure-*in*-structure morphologies with two completely different length scales, e.g., of ca. 20 and 3.6 nm, respectively.[29–31]

The P4VP(PDP) system is one example of a whole class of noncovalent side-chain polymers.[32] In the PDP case the side chains are attached by hydrogen bonding, but similar supramolecular architectures may be obtained by ionic bonding or coordination bonding.[33–36] As long as nonmesogenic flexible side chains are involved, the self-assembly can be described well by the familiar block copolymer approach; e.g., the presence of a correlation hole peak in the disordered state and its dependence on the extend of side-chain bonding can be simply discussed using the RPA approach.[37] Apart from the temperature sensitivity of the side-chain bonding, these systems also closely resemble covalent side-chain polymers such as e.g. poly(*n*-octadecyl methacrylate).[38,39] In all these cases the self-assembly results from the unfavorable side-chain/backbone interactions with a periodicity length scale that is determined by two opposing effects, i.e., minimization of interfacial area and minimization of chain stretching. If, on the other hand, mesogenic side chains are involved, a different theoretical approach is required.[40]

Noncovalent side-chain polymers incorporating azobenzene groups in the side chains have already been discussed by various groups.[41–43] Here we report on the self-assembly of P4VP hydrogen bonded with a new class of azobenzene containing amphiphiles and consider in particular the effect of the side chain length on the phase behavior. The side chains involved are not mesogenic themselves, and our discussion of the self-assembly in these systems will be similar to that used for the PDP-based systems.

Experimental Section

Materials. All the aniline derivatives were purchased form Sigma-Aldrich (purity of at least 97%) and were used as received. Phenol (99% purity) was received from Janssen Chimica and also used without further purification. Poly(4-vinylpyridine) (P4VP) was purchased from Polysciences, Inc., and had a M_w of 50 kg/mol.

Synthesis. The synthesis route to 4-(4′-alkylphenyl)azophenols is presented in Figure 1 following a recently published procedure.[44] Shown below are the basic analytical data to characterize the products obtained. For clarity, in the NMR analysis the protons in the alkyl groups are numbered alphabetically, starting with H_A for the protons at the carbon attached to the aromatic part of the molecule up to H_N for the last methyl group.

4-(4′-Hexylphenyl)azophenol (6PAP). Dark yellow solid, mp (DSC, heating, onset) 74 °C. H NMR ($CDCl_3$): $\delta = 7.86$ (*d*, 2H, H-3 and H-5), 7.79 (*d*, 2H, H-3′ and H-5′), 7.30 (*d*, 2H, H-2′ and H-6′), 6.93 (*d*, 2H, H-2 and H-6), 5.18 (*s*, 1H, −OH), 2.67 (*t*, 2H,

* To whom correspondence should be addressed. E-mail: g.ten.brinke@rug.nl.
[†] University of Groningen.
[‡] Netherlands Organization for Scientific Research.
[§] Helsinki University of Technology.

10.1021/ma800106t CCC: $40.75
Published on Web 05/20/2008

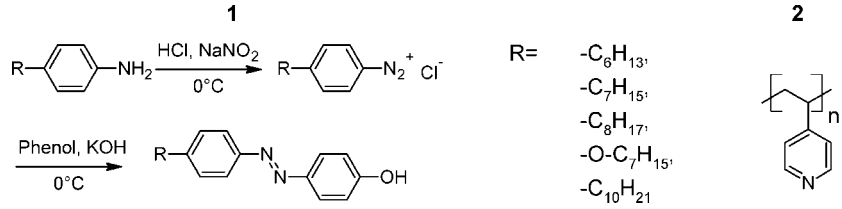

Figure 1. Chemical structures of the materials used: (1) reaction scheme of para-substituted phenylazophenol in which substituent R can be a hexyl, heptyl, octyl, heptyloxy, or decyl group; (2) poly(4-vinylpyridine).

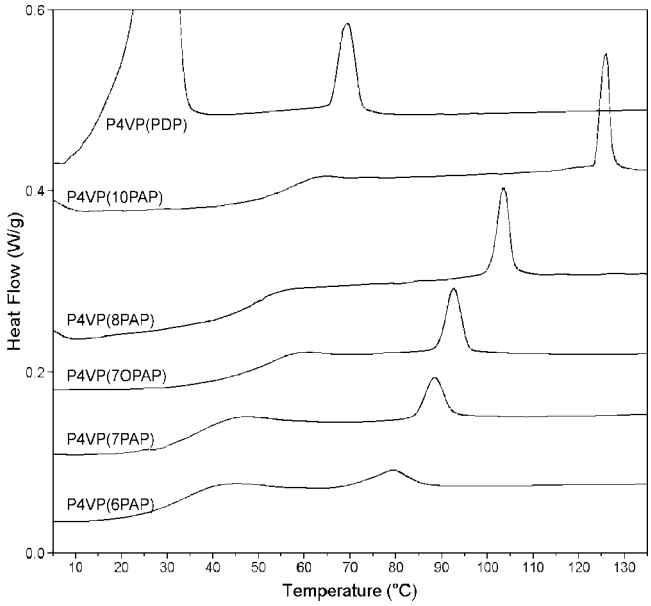

Figure 2. DSC heat flow curves of P4VP(amphiphile)$_{1.0}$ samples (exo down).

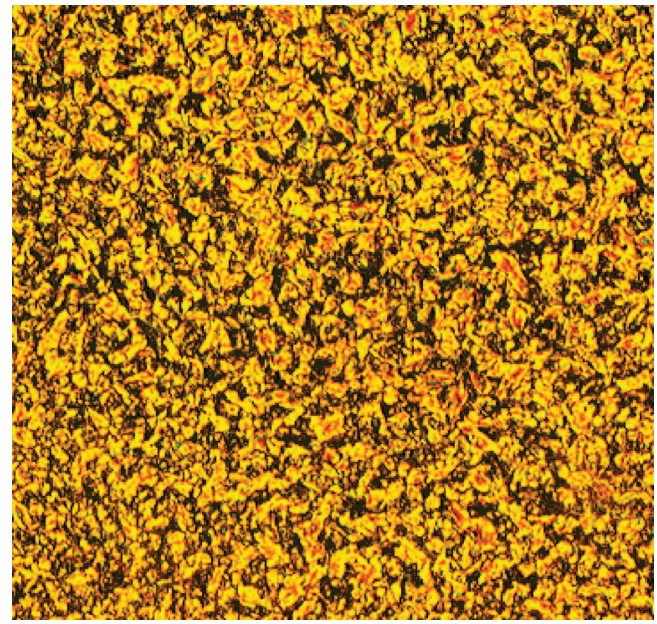

Figure 3. Polarized optical micrograph (310 × 310 μm) of P4VP(7PAP)$_{1.0}$. At temperatures above T_{ODT}, the birefringence is extinguished.

H_A), 1.67−1.31 (*m*, 10H, H_B to H_F), 0.88 (*t*, 3H, H_G). MS: *m*/*z* = 282 (calculated: 282.4).

4-(4′-Heptylphenyl)azophenol (7PAP). Dark yellow solid, mp (DSC, heating, onset) 74 °C. H NMR ($CDCl_3$): δ = 7.86 (*d*, 2H, H-3 and H-5), 7.79 (*d*, 2H, H-3′ and H-5′), 7.30 (*d*, 2H, H-2′ and H-6′), 6.94 (*d*, 2H, H-2 and H-6), 5.22 (*s*, 1H, −OH), 2.67 (*t*, 2H, H-1), 1.65−1.27 (*m*, 10H, H-2 to H-6), 0.88 (*t*, 3H, H-7). MS: *m*/*z* = 296 (calculated: 296.4).

4-(4′-Octylphenyl)azophenol (8PAP). Dark yellow solid, mp (DSC, heating, onset) 70 °C. H NMR ($CDCl_3$): 7.86 (*d*, 2H, H-3 and H-5), 7.79 (*d*, 2H, H-3′ and H-5′), 7.30 (*d*, 2H, H-2′ and H-6′), 6.94 (*d*, 2H, H-2 and H-6), 5.23 (*br s*, 1H, −OH), 2.66 (*t*, 2H, H-1), 1.65−1.28 (*m*, 12H, H-2 to H-7), 0.86 (*t*, 3H, H-8). MS: *m*/*z* = 310 (calculated: 310.4.

4-(4′-Decylphenyl)azophenol (10PAP). Dark yellow solid, mp (DSC, heating, onset) 78 °C. H NMR ($CDCl_3$): 7.86 (*d*, 2H, H-3 and H-5), 7.79 (*d*, 2H, H-3′ and H-5′), 7.30 (*d*, 2H, H-2′ and H-6′), 6.94 (*d*, 2H, H-2 and H-6), 5.25 (*br s*, 1H, −OH), 2.66 (*t*, 2H,H-1), 1.65−1.28 (*m*, 12H, H-2 to H-9), 0.86 (*t*, 3H, H-10). MS: *m*/*z* = 338 (calculated: 338.5).

4-(4′-Heptyloxyphenyl)azophenol (7OPAP). Light brown solid, mp (DSC, heating, onset) 98 °C. H NMR ($CDCl_3$): 7.86 (*d*, 2H, H-3′ and H-5′), 7.83 (*d*, 2H, H-3 and H-5), 6.97 (*d*, 2H, H-2 and H-6), 6.93 (*d*, 2H, H-2′ and H-6′), 5.19 (*br s*, 1H, -OH), 4.03 (*t*, 2H,H-1), 1.84−1.32 (*m*, 12H, H-2 to H-9), 0.90 (*t*, 3H, H-10). MS: *m*/*z* = 312 (calculated: 312.4).

Sample Preparation. The P4VP(amphiphile) systems were made by dissolving both the amphiphile and the polymer in $CHCl_3$ (p.a. grade, Aldrich) followed by leaving the solution overnight for slow evaporation in a partially covered Petri dish. Finally, the samples were dried in vacuum at 40 °C overnight. The proportion of P4VP and amphiphile was such that the amount of vinylpyridine groups in the P4VP corresponded stoichiometrically to the amount of amphiphile molecules.

Analysis Techniques. In order to determine melting temperatures T_m, order−disorder transition temperatures T_{ODT}, and glass transition temperatures T_g, differential scanning calorimetry (DSC) was performed on a DSC Q1000 (TA Instruments) using a heating rate of 10 °C/min. To eliminate the influence from the thermal history of the samples, a "heat−cool−heat" procedure was used, of which the cooling scan or the second heat scan was used for the analysis. H NMR spectra were recorded on a Varian VXR 300 MHz spectrometer using $CDCl_3$ as solvent. Mass spectrometry was conducted on a Jeol JMS 600H mass spectrometer using EI+ (70 eV) as ionization mode. Micrographs were taken on a Zeiss Axiophot equipped with a Mettler FP82HT hot stage and crossed polarizers. Small-angle X-ray scattering (SAXS) and wide-angle

Table 1. Thermal Properties of Pure Amphiphiles and P4VP(Amphiphile) Systems

	pure amphiphiles		P4VP(amphiphile)		
amphiphile	T_c, °C DSC, cooling	T_c, °C SAXS/WAXS, cooling	T_g, °C DSC, heating	T_{ODT}, °C DSC, heating	ΔH_{ODT}, J/g
10PAP	74	73	58	126	1.8
8PAP	62	61	51	103	1.8
7PAP	68	68	38	93	1.4
6PAP	63	63	34	88	1.0
7OPAP	89	89	53	80	1.6
PDP	52			69	2.3

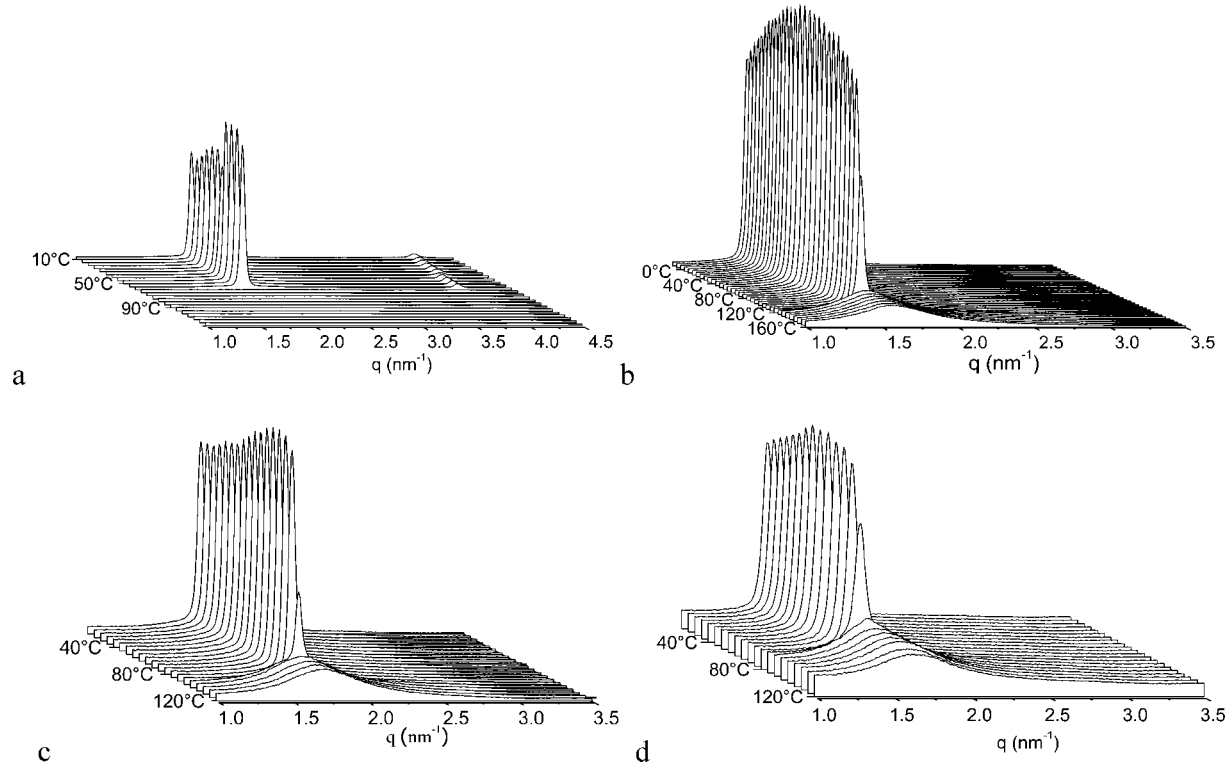

Figure 4. SAXS patterns (linear scale) as a function of temperature during cooling of (a) pure 6PAP, (b) P4VP(10PAP)$_{1.0}$, (c) P4VP(7PAP)$_{1.0}$, and (d) P4VP(7OPAP)$_{1.0}$.

Table 2. Structural Properties of the Pure Amphiphiles and P4VP(Am) Systems

amphiphile (Am)	extended length of Am, nm	periodicity crystalline Am at 20 °C, nm	periodicity P4VP(Am) at 20 °C, nm
10PAP	2.12	3.8	4.2
8PAP	2.24	3.4	3.7
7PAP	2.36	3.2	3.6
6PAP	2.61	3.0	3.3
7OPAP	2.34	3.9	4.1
PDP	2.64	2.6	3.7

X-ray scattering (WAXS) experiments were performed simultaneously at the DUBBLE beamline (BM26) at the ESRF in Grenoble, France.[45] The sample−detector distance was ca. 165 cm for SAXS and ca. 4 cm for WAXS; the X-ray wavelength was $\lambda = 1.24$ Å ($E = 10$ keV). A Linkam HFS 191 sample stage was used to heat and cool the sample with a rate of 10 °C/min. The scattering vector q is defined as $q = (4\pi/\lambda) \sin \theta$, where θ is half the scattering angle.

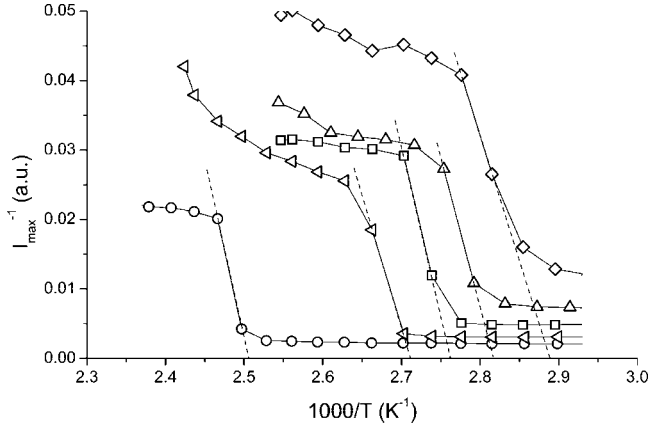

Figure 5. Plot of the inverse maximum intensity I_{max}^{-1} as a function of the reciprocal temperature (1000/T) during cooling for (○) P4VP(10PAP)$_{1.0}$, (tilted △) P4VP(8PAP)$_{1.0}$, (△) P4VP(7PAP)$_{1.0}$, (◇) P4VP(6PAP)$_{1.0}$, and (▽) P4VP(7OPAP)$_{1.0}$.

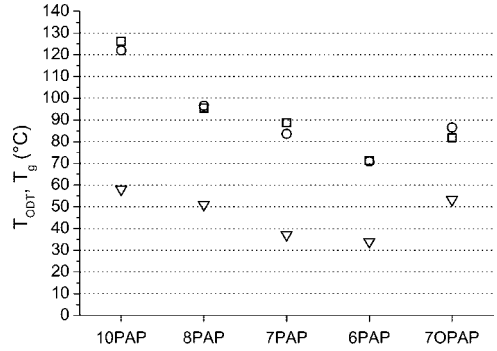

Figure 6. T_{ODT} and T_g of the P4VP(PAP) systems: (□) T_{ODT} obtained from SAXS data using the reciprocal I_{max} extrapolation procedure; (○) T_{ODT} obtained from DSC data; (▽) T_g of P4VP(PAP)$_{1.0}$ systems. Note, all ODT data presented were determined on cooling.

The measurement time per frame was 30 s, resulting in a 5 °C temperature window per frame.

Results and Discussion

Five different P4VP−amphiphile systems were investigated: four alkylphenylazophenol-based samples, denoted as P4VP-(nPAP)$_{1.0}$, where n denotes the alkyl length, $n = 6$, 7, 8, 10, and one alkyloxyphenylazophenol-based sample denoted as P4VP-(nOPAP)$_{1.0}$ with alkyl length $n = 7$. The subscript denotes the number of nPAP molecules per repeating unit. Collectively they will be denoted as P4VP(PAP). Figure 1 shows the different azophenol amphiphiles synthesized. Samples were made by solvent casting of the hydrogen-bonded complexes which for all samples resulted in orange/brown transparent films that started to crystallize after some time. SAXS experiments on the latter samples showed the presence of a crystallized phase with a scattering pattern identical to that of pure crystalline PAP. This shows that the complexes are not stable at room temperature.

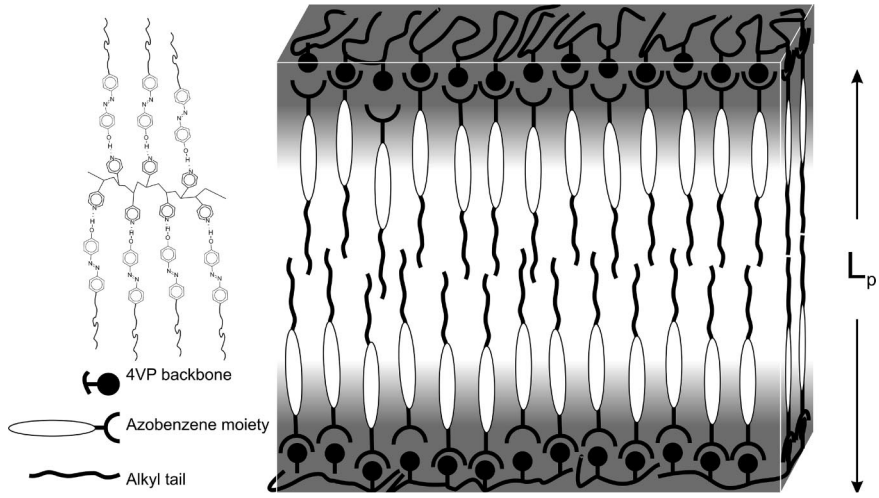

Figure 7. Schematic illustration of hydrogen bonding in P4VP(PAP) systems and the proposed lamellar phase separated structure with periodicity L_p.

To study the thermal properties of the P4VP(PAP) systems, differential scanning calorimetry was performed. The corresponding DSC curves (second heat scan) are presented in Figure 2 and show two distinct features: a glass transition and a phase transition endotherm. Compared to pure P4VP, for which $T_g \cong 150$ °C, all the P4VP(PAP) samples reveal a significant glass transition temperature reduction, by 100 °C or more. Such a T_g depression is well-known from a similar study of P4VP-based systems obtained by hydrogen bonding P4VP with pentadecylphenol (PDP) and denoted as P4VP(PDP)$_x$, where x denotes the number of PDP groups per repeat unit. Here the glass transition is not resolved in the stoichiometric complexes as it is below the crystallization temperature of the hydrogen-bonded PDP (see Figure 2). The reduction of the glass transition by adding PDP can be concluded from the less than stoichiometric complexes, e.g., for $x = 0.5$, $T_g \cong 42$ °C.[46] The endotherm corresponds, as will be shown, to an order−disorder transition from an ordered lamellar (smectic) state to a disordered melt.

The temperature values of the glass transitions and the order−disorder transitions are collected in Table 1 together with the crystallization temperatures of the pure amphiphiles and the transition enthalpy ΔH of the P4VP(nPAP) systems. The pure amphiphiles go directly from the crystalline to the isotropic melt state.

In the P4VP(PAP) samples the glass transition temperature varied from 34 °C for the shortest amphiphile (6PAP) to 58 °C for the longest amphiphile (10PAP). This counterintuitive trend in T_g reduction, longer alkyl tails leading to higher T_g values, appears to be correlated to the trend in the order−disorder transition temperature (T_{ODT}) of the P4VP(PAP) systems as given by the endothermic peak. This will be discussed in more detail further on. That the endothermic peak observed in the DSC scans (Figure 2) can be attributed to an order−disorder transition (ODT) is already quite evident from a comparison with the corresponding DSC scan of P4VP(PDP)$_{1.0}$, also presented. As seen from Table 1, for all the samples the enthalpy of the transition is similar in the range of 1−2 J/g. That the ordered state is smectic is confirmed by the polarized optical micrographs, a characteristic example being shown in Figure 3, together with the SAXS data that will be discussed further on.

It should be realized that during the second scan there is no crystallinity in the sample as confirmed by WAXS data that were collected simultaneously with the SAXS data. The transition temperatures of the different samples depend strongly on the alkyl length in a manner that is consistent with the fact that a longer alkyl chain increases the total repulsion between the alkyl side chains and the rest of the system simply because the composition expressed in volume fraction alkyl chains becomes more symmetric.

The results of the SAXS experiments as a function of temperature for the pure amphiphile 6PAP and a number of representative P4VP(PAP) samples are shown in Figure 4. The most relevant data are collected in Table 2.

The SAXS patterns of all the supramolecules samples measured on cooling from the disordered melt state are characterized by a high-temperature shallow correlation hole peak that turns into a sharp q^* scattering peak below the order−disorder temperature T_{ODT}. The correlation hole peak is directly related to the comblike architecture of the hydrogen-bonded complex and thus obviously absent for the pure amphiphiles (see Figure 4a). In all cases the position of the correlation hole peak in the disordered state is quite temperature insensitive in the sense that its position and height are still almost the same at temperatures that are 50−100 °C above the T_{ODT}. This implies that the number of hydrogen bonds in all the systems considered remains high at elevated temperatures since a significant reduction in this number is accompanied by a shift of the correlation hole peak to smaller angles and a reduction in peak height.[37]

The long periods $2\pi/q^*$ of the mesomorphic structures are collected in Table 2. For the P4VP(10PAP)$_{1.0}$ system a second-order peak at $2q^*$ is also visible, albeit very weak, thus indicating a lamellar (smectic) structure. The near absence of a second-order peak may in principle result from symmetry, but since it is invariably observed for all the systems we studied, including the P4VP(PDP) systems with different amounts of PDP, it is most likely due to the fact that the lamellar (smectic) structure formed has a large short-range disorder.[47,48]

The order−disorder transition temperatures were estimated from the SAXS data by applying the procedure illustrated in Figure 5. The reciprocal maximum intensity of the q^*-peak I_{max}^{-1} is plotted as a function of the reciprocal temperature and the tangent at the inflection point extrapolated to $I_{max}^{-1} = 0$.[49−51] Since every frame of the SAXS measurements during heating and cooling encompasses a 5 °C temperature interval, the ODT temperatures obtained in this manner are only an approximation. The transition temperatures obtained in this way are presented in Figure 6 together with the values obtained by DSC on cooling. As found before by DSC, the SAXS data demonstrate that using alkyl derivatives with a longer alkyl chain results in a higher order−disorder transition temperature.

The long periods of the P4VP(PAP) systems are presented in Table 2 and show a systematic increase as a function of the alkyl length of the nPAP used. The average increase in long period is 0.22 nm per additional CH_2 group, which is slightly

smaller than the increase in length of the all trans conformation of ca. 0.25 nm per 2 CH_2 units. Since the alkyl tails will obviously not be in the all-trans conformation, this indicates that the structure formed must be close to an end-to-end double layer, maybe with some interdigitation of the alkyl tails, as illustrated in Figure 7. Table 2 also contains the extended lengths of the amphiphiles, as evaluated from standard bond angles and bond lengths. A comparison of these with the long periods of the P4VP(*n*PAP) systems also supports an end-to-end double-layer structure. Such a structure is well-known from many other (covalent and noncovalent) side-chain polymer systems,[34,39,52] including P4VP(PDP).[51] A striking difference between the *n*PAP amphiphiles on the one hand and pentadecylphenol on the other is the strong increase in periodicity going from the crystalline state of pure PDP to the smectic P4VP(PDP) complex, respectively 2.6 and 3.7 nm (Table 2). For PDP this difference is about 1.1 nm, whereas for the PAP amphiphiles it varies from 0.2 to 0.4 nm only. Apparently, in the crystalline state pure PDP forms an interdigitated monolayer, whereas the pure *n*PAP amphiphiles form some kind of double layer.

Now we return to the trend in T_g values observed as a function of the alkyl length. The cartoon presented in Figure 7 schematically indicates the kind of smectic A layered structure that we expect to be formed. Although we cannot really exclude a smectic C structure, it is corroborated by the temperature insensitivity of the long period found for the P4VP(PAP) complexes.[53] The cartoon itself is somewhat misleading in the sense that it suggests a strongly segregated state. In reality, on cooling just below the transition temperature, the system will most likely be in a weakly segregated state. The T_g's found in these systems are due to the vitrification of the P4VP containing layers. The fact that the values found are of the order of 100 °C or more below that of pure P4VP indicates that the presence of the side chains leads to a very strong T_g depression in the already microphase-separated state, and hence, the mobility of the P4VP containing layers is strongly enhanced compared to pure P4VP due to the presence of the side chains. This suggests that the P4VP containing domains are, at least at temperatures relatively close to T_{ODT}, far from pure P4VP. It is now relatively straightforward to rationalize the trend in T_g behavior as a function of the alkyl chain length observed. Longer alkyl chains lead to an increased total repulsion and hence to a higher T_{ODT}. The higher order−disorder temperature in turn implies that at any specific temperature below T_{ODT}, e.g. room temperature, the segregation will be stronger for the systems with the longer alkyl chain lengths. As a consequence, vitrification will occur at higher temperatures for the systems with longer alkyl chain lengths.

In conclusion, we have demonstrated that 4-(4′-alkylphenyl) azophenols and 4-(4′-alkoxyphenyl)azophenols are suitable amphiphiles to create comb-shaped supramolecules with self-assembling properties similar to that of the much studied P4VP(PDP)$_x$ supramolecular systems. The azobenzene moiety in the side chain potentially introduces additionally photophysical properties to the systems, and the realization of those properties to create responsive materials is the subject of our ongoing research.

References and Notes

(1) Chen, G. H.; Hoffman, A. S. *Nature (London)* **1995**, *373*, 49–52.
(2) Lowe, A. B.; McCormick, C. L. *Prog. Polym. Sci.* **2007**, *32*, 283–351.
(3) Luzinov, I.; Minko, S.; Tsukruk, V. V. *Prog. Polym. Sci.* **2004**, *29*, 635–698.
(4) Urban, M. W. *Polym. Rev.* **2006**, *46*, 329–339.
(5) Wilson, A. J. *Soft Matter* **2007**, *3*, 409–425.
(6) Bromberg, L.; Temchenko, M.; Hatton, T. A. *Langmuir* **2003**, *19*, 8675–8684.
(7) Kwon, I. C.; Bae, Y. H.; Kim, S. W. *Nature (London)* **1991**, *354*, 291293.
(8) Miyata, T.; Uragami, T.; Nakamae, K. *Adv. Drug Delivery Rev.* **2002**, *54*, 79–98.
(9) Roy, I.; Gupta, M. N. *Chem. Biol.* **2003**, *10*, 1161–1171.
(10) Saitoh, T.; Sekino, A.; Hiraide, M. *Chem. Lett.* **2004**, *33*, 912–913.
(11) Sivakova, S.; Bohnsack, D. A.; Mackay, M. E.; Suwanmala, P.; Rowan, S. J. *J. Am. Chem. Soc.* **2005**, *127*, 18202–18211.
(12) Stoeber, B.; Yang, Z. H.; Liepmann, D.; Muller, S. J. *J. Microelectromech. Syst.* **2005**, *14*, 207–213.
(13) Sui, Z. J.; Schlenoff, J. B. *Langmuir* **2004**, *20*, 6026–6031.
(14) Fujiwara, N.; Asaka, K.; Nishimura, Y.; Oguro, K.; Torikai, E. *Chem. Mater.* **2000**, *12*, 1750–1754.
(15) Hu, Z. B.; Chen, Y. Y.; Wang, C. J.; Zheng, Y. D.; Li, Y. *Nature (London)* **1998**, *393*, 149–152.
(16) Lonergan, M. C.; Severin, E. J.; Doleman, B. J.; Beaber, S. A.; Grubb, R. H.; Lewis, N. S. *Chem. Mater.* **1996**, *8*, 2298–2312.
(17) Xie, A. F.; Granick, S. *Macromolecules* **2002**, *35*, 1805–1813.
(18) Iftime, G.; Natansohn, A.; Rochon, P. *Macromolecules* **2002**, *35*, 365–369.
(19) Ikeda, T. *J. Mater. Chem.* **2003**, *13*, 2037–2057.
(20) Ikeda, T.; Tsutsumi, O. *Science* **1995**, *268*, 1873–1875.
(21) Kato, T.; Hirota, N.; Fujishima, A.; Frechet, J. M. J. *J. Polym. Sci., Part A: Polym. Chem.* **1996**, *34*, 57–62.
(22) Natansohn, A.; Rochon, P. *Chem. Rev.* **2002**, *102*, 4139–4175.
(23) Priimagi, A.; Cattaneo, S.; Ras, R. H. A.; Valkama, S.; Ikkala, O.; Kauranen, M. *Chem. Mater.* **2005**, *17*, 5798–5802.
(24) Priimagi, A.; Kaivola, M.; Rodriguez, F. J.; Kauranen, M. *Appl. Phys. Lett.* **2007**, *90*, 121103.
(25) Shibaev, V.; Bobrovsky, A.; Boiko, N. *Prog. Polym. Sci.* **2003**, *28*, 729–836.
(26) Yu, H. F.; Asaoka, S.; Shishido, A.; Iyoda, T.; Ikeda, T. *Small* **2007**, *3*, 768–771.
(27) Ruokolainen, J.; ten Brinke, G.; Ikkala, O.; Torkkeli, M.; Serimaa, R. *Macromolecules* **1996**, *29*, 3409–3415.
(28) Ruokolainen, J.; Torkkeli, M.; Serimaa, R.; Komanschek, B. E.; Ikkala, O.; ten Brinke, G. *Phys. Rev. E* **1996**, *54*, 6646–6649.
(29) ten Brinke, G.; Ruokolainen, J.; Ikkala, O. *Adv. Polym. Sci.* **2007**, *207*, 113–177.
(30) Ikkala, O.; ten Brinke, G. *Science* **2002**, *295*, 2407–2409.
(31) Ruokolainen, J.; Makinen, R.; Torkkeli, M.; Makela, T.; Serimaa, R.; ten Brinke, G.; Ikkala, O. *Science* **1998**, *280*, 557–560.
(32) Pollino, J. M.; Weck, M. *Chem. Soc. Rev.* **2005**, *34*, 193–207.
(33) Antonietti, M.; Conrad, J.; Thünemann, A. *Macromolecules* **1994**, *27*, 6007–6011.
(34) Ober, C. K.; Wegner, G. *Adv. Mater.* **1997**, *9*, 17–31.
(35) Ruokolainen, J.; Tanner, J.; ten Brinke, G.; Ikkala, O.; Torkkeli, M.; Serimaa, R. *Macromolecules* **1995**, *28*, 7779–7784.
(36) Thünemann, A. F. *Prog. Polym. Sci.* **2002**, *27*, 1473–1572.
(37) Huh, J.; Ikkala, O.; ten Brinke, G. *Macromolecules* **1997**, *30*, 1828–1835.
(38) Hempel, E.; Budde, H.; Höring, S.; Beiner, M. In *Progress in Understanding of Polymer Crystallization*; Springer: Berlin, 2007.
(39) Platé, N. A.; Shibaev, V. P. *Comb-like Polymers and Liquid Crystals*; Plenum Press: London, 1987.
(40) Warner, M. *Side Chain Liquid Crystal Polymers*; Chapman & Hall: New York, 1989; pp 7−28.
(41) Ujiie, S.; Iimura, K. *Macromolecules* **1992**, *25*, 3174–3178.
(42) Sallenave, X.; Bazuin, C. G. *Macromolecules* **2007**, *40*, 5326–5336.
(43) Sun, K.; Liu, J.; Gao, J. G.; Su, W.; Zhang, D. G.; Wang, P.; Zhang, Q. J. *J. Polym. Sci., Part B: Polym. Phys.* **2006**, *44*, 1378–1384.
(44) Suwanprasop, S.; Suksorn, S.; Nhujak, T.; Roengsumran, S.; Petsom, A. *Ind. Eng. Chem. Res.* **2003**, *42*, 5054–5059.
(45) Bras, W.; Dolbnya, I. P.; Detollenaere, D.; van Tol, R.; Malfois, M.; Greaves, G. N.; Ryan, A. J.; Heeley, E. *J. Appl. Crystallogr.* **2003**, *36*, 791–794.
(46) Luyten, M. C.; van Ekenstein, G. O. R. A.; ten Brinke, G.; Ruokolainen, J.; Ikkala, O.; Torkkeli, M.; Serimaa, R. *Macromolecules* **1999**, *32*, 4404–4410.
(47) Mcmillan, W. L. *Phys. Rev. A* **1971**, *4*, 1238–&000.
(48) Stamatoff, J.; Cladis, P. E.; Guillon, D.; Cross, M. C.; Bilash, T.; Finn, P. *Phys. Rev. Lett.* **1980**, *44*, 1509–1512.
(49) Ehlich, D.; Takenaka, M.; Hashimoto, T. *Macromolecules* **1993**, *26*, 492–498.
(50) Hashimoto, T.; Shibayama, M.; Kawai, H. *Macromolecules* **1983**, *16*, 1093–1101.
(51) Luyten, M. C.; van Ekenstein, G. O. R. A.; Wildeman, J.; ten Brinke, G.; Ruokolainen, J.; Ikkala, O.; Torkkeli, M.; Serimaa, R. *Macromolecules* **1998**, *31*, 9160–9165.
(52) Percec, V.; Pugh, C. In *Side Chain Liquid Crystal Polymers*; McArdle, C. B., Ed.; Chapman and Hall: New York, 1989; Chapter 3.
(53) Gray, G. W.; Goodby, J. W. *Smectic Liquid Crystals*; Leonard Hill: Glasgow, 1984.

MA800106T